NMDA induces post-transcriptional regulation of α_2-guanylyl-cyclase-subunit expression in cerebellar granule cells

Sandra Jurado[1], Fernando Rodríguez-Pascual[2], José Sánchez-Prieto[1], Francisco M. Reimunde[2], Santiago Lamas[2] and Magdalena Torres[1,*]

[1]Departamento de Bioquímica, Facultad de Veterinaria, Universidad Complutense, Madrid, E-28040 Spain
[2]Centro de Investigaciones Biológicas (CIB), Consejo Superior de Investigaciones Científicas (CSIC), Ramiro de Maeztu 9, Madrid, E-28040 Spain
*Author for correspondence (e-mail: mitorres@vet.ucm.es)

Accepted 4 January 2006
Journal of Cell Science 119, 1622-1631 Published by The Company of Biologists 2006
doi:10.1242/jcs.02867

Summary

Activation of N-methyl-D-aspartate (NMDA) glutamate receptors commonly affects gene expression in different neurons. We reported previously that chronic treatment of rat cerebellar granule cells with NMDA (24 hours) upregulates the expression of mRNA encoding the α_2 subunit of the nitric-oxide-sensitive guanylyl cyclase. However, the molecular mechanisms involved in this process remained to be elucidated. Here, we have performed mRNA-decay experiments using the transcriptional inhibitor actinomycin D, providing evidence that the half-life of α_2 mRNA is significantly prolonged in cells exposed to NMDA. The role of the 3′ untranslated region of the α_2 transcripts in NMDA-induced mRNA stabilisation was examined and an association between the RNA-binding proteins AUF1 and ELAV-like protein 1 (HuR/HuA), and endogenous α_2 mRNA was demonstrated in vivo, as revealed by coimmunoprecipitation experiments with specific antibodies against AUF1 and HuR. Further studies indicated that stimulation of the NMDA receptor induces a downregulation in AUF1 levels stabilising the α_2 mRNA transcripts. These events are triggered through a mechanism that depends on formation of nitric oxide, and on the subsequent activation of guanylyl cyclase and cGMP dependent protein kinases.

Key words: AUF1, Cerebellar granule cells, mRNA decay, NO-sensitive guanylyl cyclase, N-methyl-D-aspartate

Introduction

Cerebellar granule cells express both Ca^{2+} permeable N-methyl-D-aspartate (NMDA) and non-NMDA glutamate receptors (Garthwaite et al., 1986; Meier and Jorgensen, 1986; Pearce et al., 1987). Indeed, stimulation of NMDA receptors in these cells is essential for survival and differentiation during their development, and it also plays a fundamental role in neuroplasticity (Kleinschmidt et al., 1987; Balazs et al., 1988; Bessho et al., 1994; Contestabile, 2000). Formation of nitric oxide (NO) is one consequence of NMDA receptor stimulation (Garthwaite and Boulton, 1995) and because neuronal NO synthase (nNOS) is anchored to NMDA receptors through the postsynaptic density protein 95 (PSD-95), Ca^{2+} entry through these receptors activates nNOS (Brenman et al., 1996; Craven and Bredt, 1998; Sheng and Pak, 2000). Hence, it has been proposed that NO acts as a messenger during development and synaptic plasticity, as well as in the cell-death process that can also be initiated through NMDA-receptor activation (Dawson et al., 1993; Bredt and Snyder, 1994; Holscher, 1997; Contestabile, 2000). What is more, the activity of this receptor dynamically regulates nNOS expression in the cerebellum and in cerebellar granule cells (Baader and Schilling, 1996; Virgili et al., 1998), and mRNA expression of NO-activated guanylyl cyclase subunits in cultured granule cells, the mRNA of the α_2 subunit being the most strongly regulated (Jurado et al., 2003). It is thought that the expression of nNOS in developing cerebellar granule cells is regulated by excitatory neurotransmission and that Ca^{2+} is an important signal transduction molecule involved in this regulatory process (Baader and Schilling, 1996). Nevertheless, the mechanism by which NMDA augments the expression of the α_2 subunit mRNA in granule cells remains to be elucidated.

Post-transcriptional gene regulation, particularly events affecting mRNA stability, are emerging as crucial factors in the regulation of gene expression (Sachs, 1993). Although the mechanisms determining mRNA turnover are poorly understood, they are generally believed to involve the recognition of specific sequences by RNA-binding proteins. The best characterised RNA sequences involved in stabilising mRNA are the AUUUA-motifs (AU-rich elements, AREs). These elements are usually found in the 3′ untranslated regions (3′ UTR) of mRNAs, such as those encoding cytokines and growth factors (Chen and Shyu, 1995; Xu et al., 1997). To date, such sequences have been found in many different mRNAs, including several components of the NO-cGMP pathway, the activities of which are known to be regulated by altering mRNA stability, e.g. α_1 and β_1 subunits of guanylyl cyclase in rat aorta (Klöss et al., 2003; Klöss et al., 2004), NO synthase II in human mesangial cells (Pérez-Sala et al., 2001), and in human intestinal epithelium (DLD1) cells (Rodríguez-Pascual

et al., 2000). The stability of a particular mRNA species is controlled by specific interactions between its structural elements and RNA-binding proteins (Guhaniyogi and Brewer, 2001). The most extensively studied RNA-binding proteins that stabilise or destabilise different mRNAs are the AUF1 proteins and the ELAV (embryonic-lethal abnormal vision)-like family that is comprised of four members: HuD (ElrD), HuC (ElrC, and ple21), He1-N1 (HuB, Mel-N1 and ElrB) and HuR (HuA and ErlA) (Fan and Steitz, 1998; Peng et al., 1998; Akamatsu et al., 1999; Bhattacharya et al., 1999; Lal et al., 2004).

The aim of the present study was to characterise the molecular mechanisms underlying the upregulation of α_2 guanylyl cyclase subunit mRNA following stimulation of NMDA receptors in cultured cerebellar granule cells. We observed that the 3′ UTR of α_2 mRNA is very long and that it contains several AREs that are targets of *elav* family members and AUF1 proteins. Furthermore, we show that exposure to NMDA increases α_2 mRNA stability by decreasing the levels of AUF1 proteins through a mechanism that requires NO and cGMP synthesis, as well as the activation of a cGMP-dependent protein kinase.

Results

NMDA treatment increases the stability of mRNA transcripts encoding the α_2 subunit of guanylyl cyclase in cerebellar granule cells

We measured the amount of mRNA encoding the α_2 subunit of guanylyl cyclase in granule cells when stimulated by NMDA. A time-dependent increase in the accumulation of α_2 guanylyl cyclase mRNA transcripts was observed in the presence of NMDA. Indeed, the amount of mRNA progressively augmented during the exposure to NMDA until reaching a maximum at 24 hours of treatment. From this point onwards, continued exposure to NMDA produced a decrease in the levels of α_2 mRNA (Fig. 1).

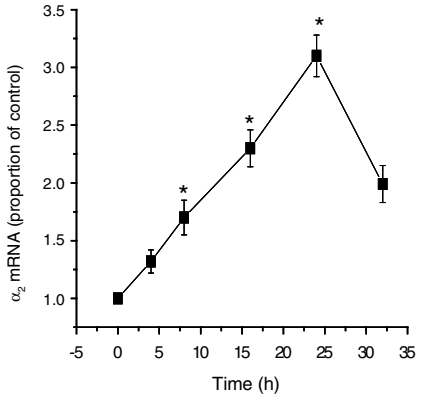

Fig. 1. Time-course of the upregulation of guanylyl cyclase α_2 mRNA induced by NMDA in cerebellar granule cells. NMDA 100 μM was added to the culture medium and the total RNA extracted at the time points indicated. The RNA was reverse transcribed using random hexamers and the amount of α_2 mRNA and 18S rRNA was determined by quantitative PCR using specific primers and probes for both. All the results were normalised against the 18S rRNA values and represent the mean ± s.e.m. of three experiments performed in triplicate. **P*<0.001, significant difference from control values.

These results raised the question whether the upregulation of α_2 mRNA upon exposure to NMDA depends on transcription or translation. To address this, we analysed the effect of NMDA in the presence of actinomycin D or cycloheximide, which inhibit transcription and translation, respectively. When granule cells that had been 7 days in vitro (7-DIV) were incubated in the presence of 50 μM NMDA for 24 hours, the amount of α_2 mRNA increased threefold (Fig. 2A). Likewise, when translation was blocked by the addition of 5 μg/ml cycloheximide, the amount of α_2 mRNA also increased approximately threefold, although the subsequent

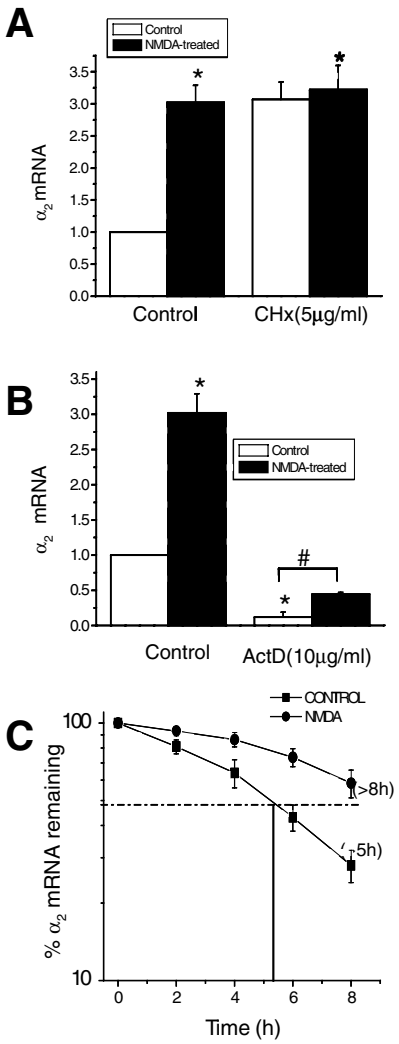

Fig. 2. (A,B) Effect of (A) cycloheximide (CHx) and (B) actinomycin D (ActD) on the activity of NMDA. Cells were incubated with the concentrations of actinomycin D or CHx indicated for 30 minutes before the addition of NMDA. The mRNA was then extracted 24 hours later and subjected to RT-PCR (using random hexamers) and quantitative PCR. The results are the mean ± s.e.m. of five experiments performed in triplicate. **P*<0.001 and #*P*<0.001, significant difference from control values. (C) The half-life of α_2 mRNA was assessed in control and NMDA-treated cells by using actinomycin D (10 μg/ml). RNA was harvested at selected time points and the relative abundance of α_2 mRNA was determined by quantitative RT-PCR. The results are the mean ± s.e.m. of four experiments performed in triplicate.

addition of NMDA did not produce a further increase in transcript levels. However, none of these treatments modified the total amount of RNA (control cells 10.65±0.95 μg/5×10^6 cells; NMDA-treated cells 9.90±0.63 μg/5×10^6 cells; cycloheximide-treated cells 9.4±1.26 μg/5×10^6 cells). Whereas the inhibition of transcription with actinomycin D led to an approximately eightfold decrease in the amount of α_2 mRNA, NMDA was still capable of producing a threefold increase in these levels (Fig. 2B). These results suggest that the effect of NMDA does not depend on translation and augments the abundance of α_2 mRNA by decreasing its degradation rate because the accumulation of a particular mRNA species is the result of the equilibrium between the rate of synthesis and the rate of degradation. Moreover, it has been shown that inhibition of protein synthesis increases AREs-containing mRNA stability in different systems (Altus et al., 1987; Oliveira and McCarthy, 1995; Ross, 1995; Guhaniyogi and Brewer, 2001) and, here, we observed an increase in α_2 mRNA after cycloheximide treatment. To determine whether the stability of α_2 mRNA is affected by NMDA, control and NMDA-treated cells were incubated in the presence of actinomycin D for different periods of time and the amount of α_2 transcripts was measured. In control cells, the amount of α_2 mRNA dropped to 50% after a 5-hour treatment with actinomycin D (Fig. 2C). However, 58% of the initial amount of α_2 mRNA remained after an 8-hour actinomycin D addition in NMDA-treated cells. As such, it appeared that NMDA might indeed increase the level of α_2 mRNA by decreasing the degradation rate of this transcript.

α_2 mRNA has a long 3′ UTR that contains several AU-rich sequences

It is becoming clear that determinants in the 3′ UTR of mRNA transcripts control aspects of their degradation. In different mRNAs, AREs present in the 3′ UTR influence the stability of the mRNA transcripts, because the proteins that bind to these elements interact with, and stabilise or destabilise them. The 3′ UTR of the rat α_2 subunit of guanylyl cyclase had not been sequenced previously. Therefore, the 3′ flanking region of sGC α_2 mRNA from cerebellar granule cells was cloned and sequenced, in order to characterise the sGC 3′ UTR in α_2 transcripts. An oligonucleotide was designed into the coding region (F1; Fig. 3A), which, when used in combination with the oligonucleotide (R1), amplified a fragment of 843 bp. This fragment was amplified from mRNA because it was not detected in the absence of reverse transcriptase and, thus, was not amplified from contaminating DNA (Fig. 3B). The combination of a second pair of primers, Forward 2 (F2) and Reverse 2 (R2; Fig. 3A), amplified a 1176 bp fragment of the mRNA (Fig. 3B). The PCR products were sequenced and subcloned into the vector pCR®II, and their identity was confirmed by restriction analysis (results not shown). The two fragments amplified were overlapping, the complete fragment corresponding to the 3′ UTR of α_2 mRNA being 1873 bp long (GenBank accession number AY795577). However, we believe the complete 3′ UTR is 100-150 bp longer because the PCR fragment obtained by using the Forward 2 and an oligo-dT primer is larger than the fragment obtained with the F2-R2 primer pair (Fig. 3B). Although we did not clone or sequence these additional 100-150 bp, it is clear that the sGC α_2 mRNA has a 3′ UTR of about 2000 bp and bears many AU-rich motifs

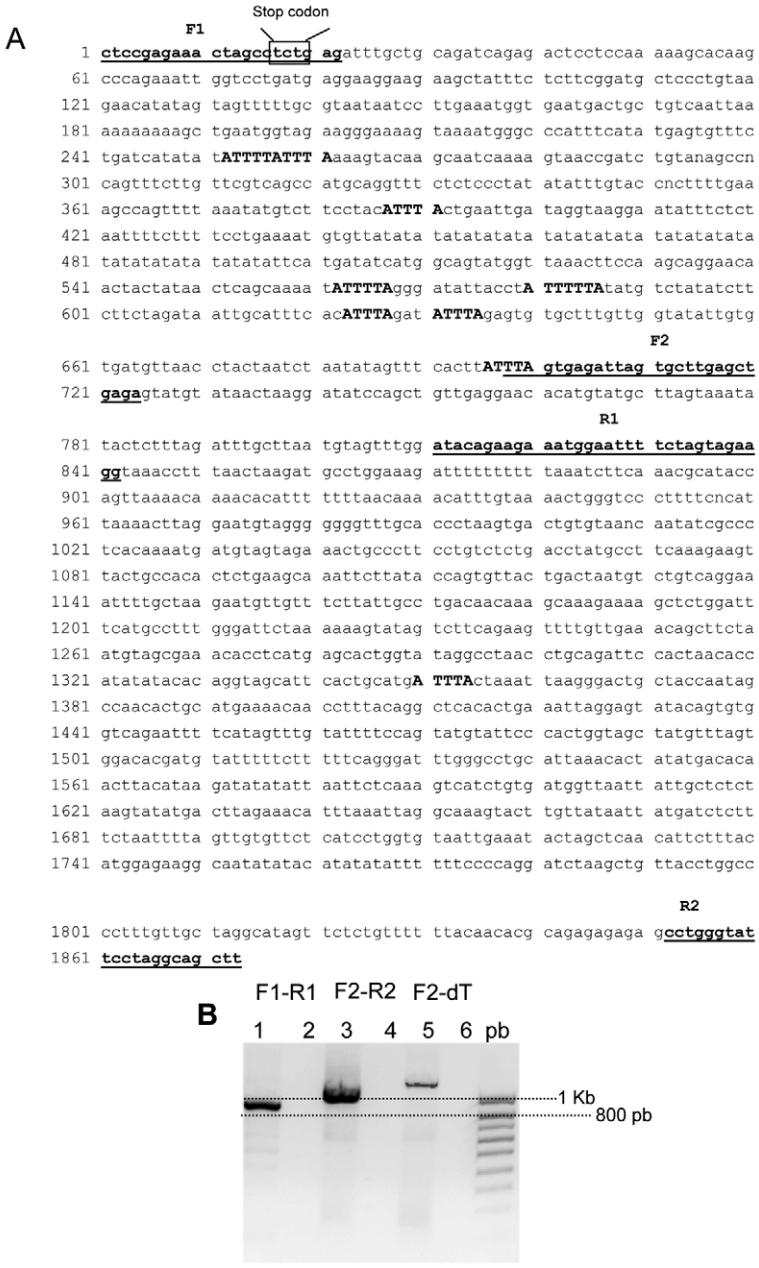

Fig. 3. (A) 3′ UTR sequence of α_2 mRNA. This sequence was obtained by direct sequencing and by cloning and sequencing of two overlapping PCR fragments. The two oligonucleotide pairs for PCR are indicated in bold and underlined, and are labelled as F1, R1 and F2, R2. ARE sequences are indicted in bold capital letters. (B) An agarose gel showing the PCR products obtained with the different oligonucleotide pairs. Lanes 1, 3 and 5 correspond to the PCR products obtained after RT. Lanes 2, 4 and 6 show that no amplification was observed in the absence of RT; dT, oligodT.

that could be targets for the binding of proteins that stabilise or destabilise the mRNA.

Binding of synthetic RNA probes to the α_2 3′ UTR in nuclear extracts from granule cells

The 3′ UTR fragments we had isolated were employed to synthesise radiolabelled RNA probes to perform RNA-protein binding assays. These binding assays were carried out on nuclear or cytosolic extracts from granule cells, with RNA probes generated from both the 843 bp fragment (probe I) and the 1176 bp fragment (probe II). Protein-RNA complexes were detected in these assays when probe I was incubated with nuclear extracts (from Fig. 4A, lanes 3 and 5; Fig. 4B, lanes 2 and 3), but not when this RNA probe was incubated with the same amount of cytosolic protein (Fig. 4A, lanes 2 and 4); nor were labelled complexes observed when the experiment was performed in the presence of competing unlabelled probe (lane 4, Fig. 4B). In contrast to, we did not observe the formation of RNA-protein complexes when the same experiments were performed with probe II (Fig. 4C). These results can be explained by the concentration of most of the AU-rich elements in the sequence corresponding to probe I (as it is shown in Fig. 3).

Binding of Hu and AUF1 to endogenous mRNA transcripts encoding the α_2 subunit of guanylyl cyclase

Of the proteins that influence mRNA-turnover through their recognition of and binding to AREs, the most extensively studied are the adenosine-uridine binding factor AUF1 and members of the ELAV-like family of proteins that are also known as Hu proteins (HuA and/or R, HuB, HuC, HuD). To determine whether the AUF1 or Hu proteins bind to α_2 mRNA in vivo, these proteins were immunoprecipitated from cell extracts wih specific antibodies, and the presence of α_2 mRNA in the purified complexes was investigated. As a control of the non-specific association of mRNAs during immunoprecipitation (IP), parallel incubations were performed with IgG. In the latter, little or no material was observed after 35 cycles of PCR amplification. Control 18S rRNA was used to monitor the background of RNA-binding during IP. Again, no amplification products were observed when reverse transcriptase was omitted. The enrichment of transcripts in each sample was calculated by quantitative real-time reverse transcriptase (RT)-PCR. To quantify the amount of 18S rRNA and α_2 mRNA in each sample, the c_T (threshold cycle) values were compared with standard curves obtained from serial dilutions of a RT product and with the specific 18S and α_2 primers and probes. The relative amount of α_2 mRNA in each sample was always considered respective to the amount of 18S rRNA, which was virtually equivalent in all the samples.

In AUF1 IPs from nuclear extracts there was an 18-fold enrichment of α_2 mRNA compared to a twofold enrichment in the AUF1 IPs from the cytosolic fraction, and the nuclear HuR IPs (Fig. 4D). By contrast, there was no enrichment of α_2 mRNA in the cytosolic HuR IP. These results show that both AUF1 proteins and HuR proteins bind to α_2 mRNA in vivo, and these protein-mRNA complexes are enriched in the nuclear fraction. Although the α_2 transcripts were associated in complexes immunoprecipitated with both antibodies, α_2 mRNA was more abundant in the AUF1 protein complex. This led us to ask whether the levels of these proteins are affected by NMDA treatment, thereby explaining the effect of NMDA on α_2 mRNA stability and accumulation.

NMDA treatment leads to a decrease in the nuclear levels of AUF1

AUF1 levels were analysed in total, nuclear and cytosolic extracts obtained from both control and NMDA-treated cells. In total extracts, all four AUF1 isoforms were detected (molecular mass: 37, 40, 42 and 45 kDa), and their levels

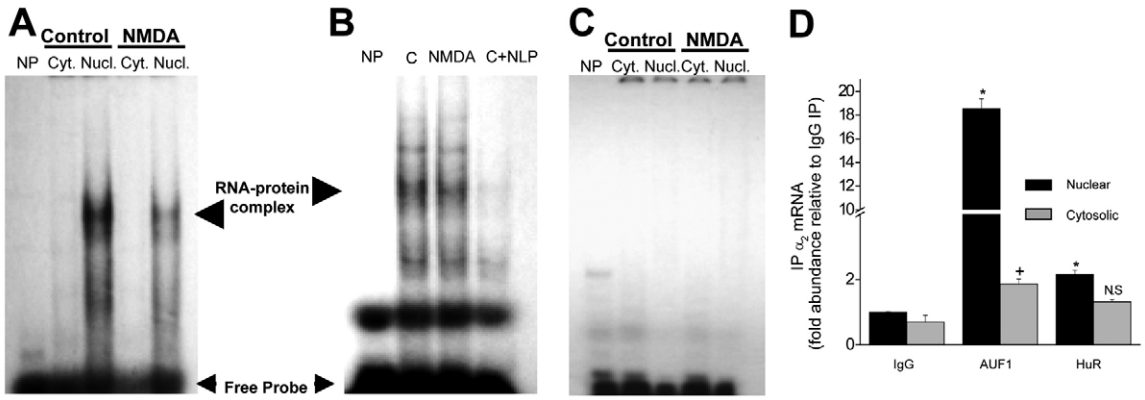

Fig. 4. Interaction of the RNA probes from the 3′ UTR of the rat α_2 subunit of guanylyl cyclase with nuclear or cytosolic proteins extracted from granule cells. (A) A radiolabelled, in vitro transcribed RNA fragment corresponding to the 843 bp fragment obtained with F1 and R1 primers (see Fig. 3) was incubated with of cytosolic (Cyt) or nuclear (Nucl) protein extracts from control or NMDA-treated cells. After binding, RNA-protein complexes were treated with T1 RNase and resolved by non-denaturing gel electrophoresis as described in the Materials and Methods. Controls were performed without the protein extract (NP). (B) Radiolabelled, in vitro transcribed RNA fragments corresponding to that of described in panel A was incubated with nuclear (Nucl) protein extracts from NMDA-treated cells or control cells, in the presence or absence of the non-labelled probe (NLP). (C) Radiolabelled, in vitro transcribed RNA fragment corresponding to the 1176 bp fragment obtained with the F2 and R2 primers (see Fig. 3) was used in a similar experiment to that described in A. (D) The presence of endogenous α_2 mRNA was assayed in the IP material from cytosolic or nuclear extracts obtained with anti-HuR or anti-AUF1 by real-time RT-PCR. The results are the mean ± s.e.m. of two experiments. $^*P<0.01$ and $^+P<0.01$, significant difference from control values (IgG).

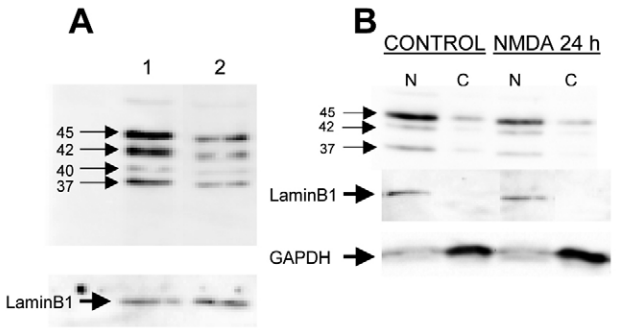

Fig. 5. NMDA-treatment downregulates AUF1 levels in granule cells. (A) Whole-cell lysate (20 μg) of (1) control or (2) NMDA-treated cells, lamin B1 was immunodetected as loading control. (B) Nuclear or cytosolic extracts (N or C, respectively) from control or NMDA-treated cells. Lamin B1 (a nuclear protein) and GAPDH were immunodetected as loading control.

decreased after NMDA treatment (with 50 or 100 μM) (Fig. 5A). When the presence of these proteins was analysed in nuclear and cytosolic extracts they were, in most experiments, clearly detected in nuclei but not in the cytosol. In some experiments AUF1 proteins were detected in the cytosolic extracts but always at very low levels (Fig. 5B). In the majority of the experiments the 40 kDa isoform was not detected, not even in nuclear extracts where the quantity of the other isoforms was very high. In cells treated with NMDA, the amount of AUF1 proteins decreased in both the nuclei and the whole-cell extract by 50%, and this reduction might be responsible for the increased stability of α_2 mRNA in response to NMDA. The level of the nuclear protein lamin B1 and the level of GAPDH, used as loading control, did not change after NMDA treatment (Fig. 5B).

NMDA decreases the AUF1 levels and increases α_2 mRNA levels by activating the NO-cGMP pathway

It is well known that, the activation of NMDA receptor permits the entry of Na^+ and Ca^{2+}, and increases in intracellular Ca^{2+} activate a wide range of intracellular cascades. One such cascade leads to the synthesis of NO and, thus, we analysed whether NMDA stimulation leads to an increase in cytosolic Ca^{2+} and in NO synthesis in our cell preparations. When 7-DIV cells were loaded with the Ca^{2+} indicator Fluo 4-AM and then stimulated with NMDA, an increase in intracellular Ca^{2+} was observed (Fig. 6A). This increase in intracellular Ca^{2+} was accompanied by an increase in NO accumulation (Fig. 6B) that was impaired by the broad-spectrum NOS inhibitor L-NAME. Thus, NMDA appears to stimulate an increase in endogenous NO synthesis. The specificity of the assay was confirmed by adding the nitric oxide donor diethylamino-diazenolate-2-oxido (DEA/NO) that overcame the inhibition of L-NAME.

The endogenous NO produced upon exposure to NMDA, stimulated guanylyl cyclase to synthesise cGMP, as observed in most cells in response to NMDA (Fig. 6C). Indeed, treatment with the cyclic nucleotide phosphodiesterase inhibitor 3-isobutyl-1-methylxanthine (IBMX) increased cGMP in the soma of granule cells and there was a big increase in cGMP after exposure to NMDA both in the soma and in the fibres of the granule cells. The synthesised cGMP could activate cGMP-dependent protein kinases in 7-DIV granules cells because in culture, these cells have been shown to express both cGMP-dependent protein kinases I and II (cGKs), (Jurado et al., 2004). Hence, it was no surprise that NMDA

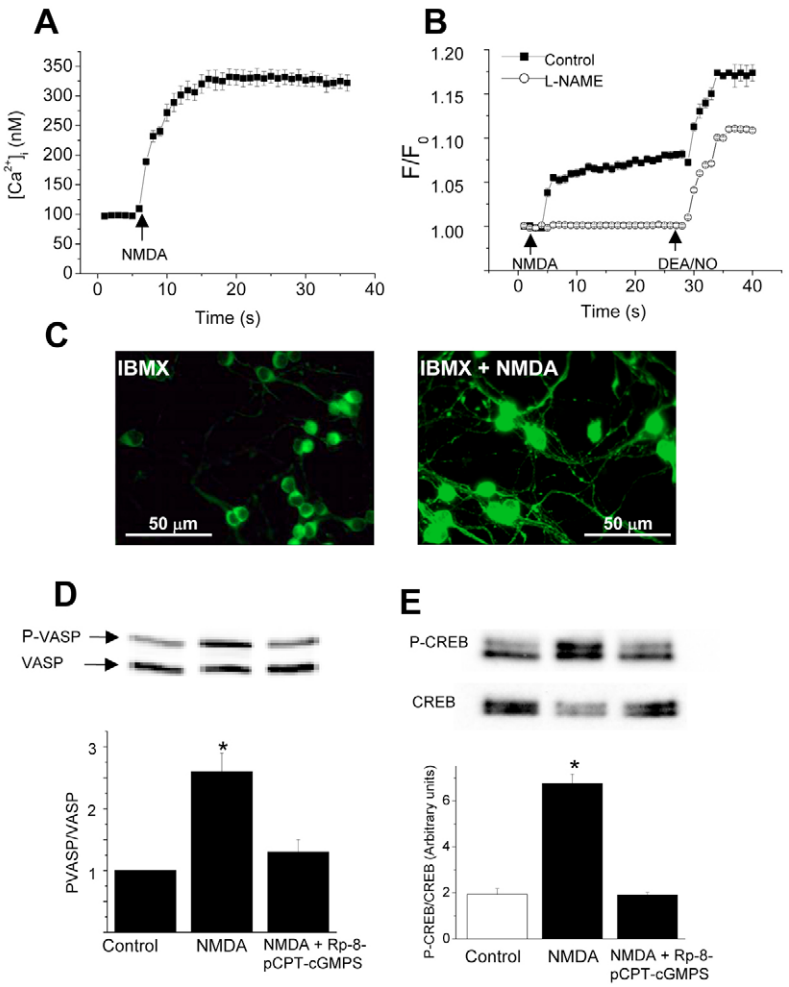

Fig. 6. NMDA stimulates the NO-cGMP pathway in granule cells. (A) NMDA increases intracellular Ca^{2+} levels, as measured with the fluorimetric probe FLUO-4AM. (B) NMDA increases intracellular NO as measured with the fluorimetric probe DAF-FM. (C-E) NMDA also stimulates (C) cGMP, (D) VASP phosphorylation and (E) CREB phosphorylation. For immunocytochemistry, cells were incubated in the presence of 0.5 mM IBMX for 30 minutes and then fixed or stimulated with 100 μM NMDA for10 minutes before processing as described in Materials and Methods.. For phosphorylation studies, cells were incubated with 100 μM NMDA for 15 minutes in the presence or absence of 20 μM Rp-8-pCPT-cGMPS added 30 minutes before the stimulation. VASP and CREB phosphorylation was analysed with specific antibodies as described in the Materials and Methods. *P<0.001, significant difference from control values.

stimulation lead to a 2.6-fold increase in VASP phosphorylation, one of the best-characterised endogenous substrates of these enzymes. This increase in VASP phosphorylation was prevented in the presence of a specific inhibitor of these kinases (Fig. 6D). NMDA stimulation also increased CREB phosphorylation, which was also prevented by Rp-8-pCPT-cGMPS (Fig. 6E). Thus, it appears that NMDA triggers the activation of the NO-cGMP pathway in cultured cerebellar granule cells.

To determine whether these signalling events are involved in the NMDA-elicited reduction of AUF1 and the increased accumulation of α_2 mRNA transcripts, the effect of NMDA on these phenomena was analysed in the presence of inhibitors of this pathway. NMDA treatment produced a 50% reduction in AUF1 protein accumulation but this effect was prevented by ODQ (10 μM) and KT5823 (1 μM), inhibitors of guanylyl cyclase and cGMP-dependent-protein kinases, respectively (Fig. 7A). Furthermore, the effect of NMDA was mimicked by Sp-8-Br-PET-cGMPS (50 μM), a cGMP analogue that activates cGKs. KT5823 not only prevented the decrease in AUF1 protein caused by NMDA but also increased AUF1 levels in non-stimulated cells (Fig. 7B), indicating that basal cGK activity is controlling AUF1 levels. Since the downregulation of AUF1 levels by NMDA involves a mechanism that depends on activation of the NO-cGMP pathway, we determined whether these compounds also affected the NMDA-elicited upregulation of α_2 mRNA. Indeed, the presence of the guanylyl cyclase inhibitor ODQ or of the cGK inhibitor KT5823 impaired accumulation of α_2 mRNA transcripts induced by the NMDA receptor, as did the NMDA receptor antagonist MK801 (Fig. 7C). When the effect of these compounds was analysed in cells that had not been not stimulated with NMDA, ODQ produced a slight but not statistically significant decrease in α_2 mRNA. However, in cells incubated with KT5823 the α_2 mRNA amount was reduced by 40%. Conversely, in cells treated with Sp-8-Br-PET-cGMPS α_2 mRNA increased 2.75-fold.

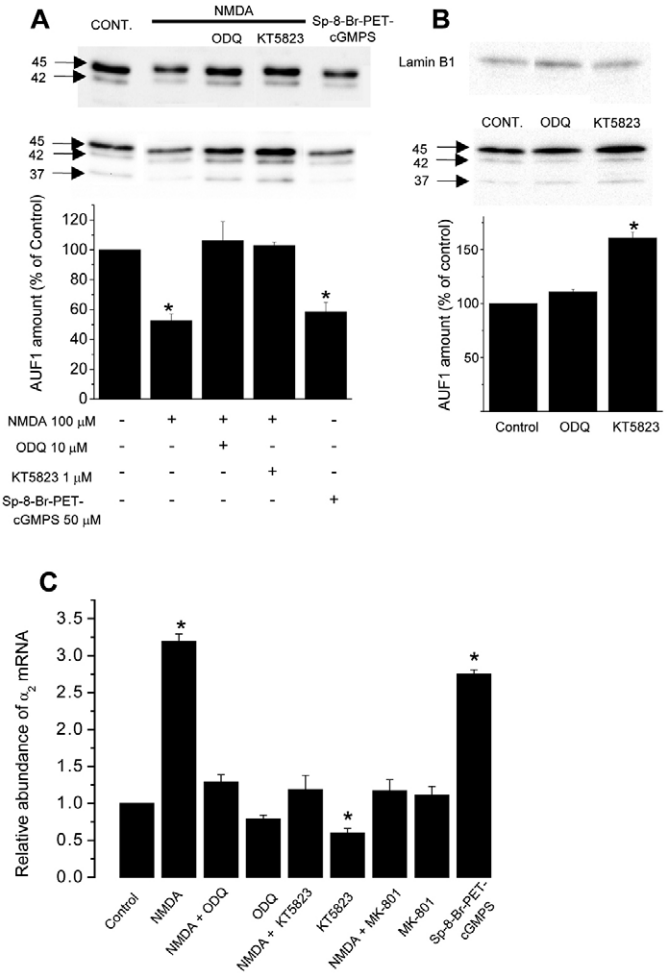

Fig. 7. (A-C) Specific inhibitors of the NO-cGMP pathway (B) affect nuclear AUF1 levels and (A) abolish the effects of NMDA on nuclear AUF1 levels and on (C) the accumulation of α_2 mRNA. Cells were incubated with the indicated compounds alone or in combination with 100 μM NMDA for 24 hours (ODQ and KT5823 were added 30-60 minutes before NMDA). Subsequently, proteins or RNA were extracted and processed as described in the Materials and Methods. (KT5823, 1 μM; MK-801, 5 μM; ODQ, 10 μM; and Sp-8-Br-PET-cGMPS, 50 μM). The results are the mean ± s.e.m. of four experiments. *P<0.001, significant difference from control values.

Discussion

Treatment with NMDA increased the accumulation of mRNA encoding different subunits of NO-sensitive guanylyl cyclase, the transcript encoding the α_2 subunit being the most affected (Jurado et al., 2003). Whereas different mechanisms have been proposed to regulate the expression of the α_1 and β_1 subunits of guanylyl cyclase in different cell types (Ferrero et al., 2000; Ferrero and Torres, 2002; Klöss et al., 2003; Klöss et al., 2004), no studies on the regulation of α_2 expression have been carried out to date. This is surprising, given that this subunit seems to be responsible for the synaptic localisation of guanylyl cyclase (Russwurm et al., 2001), which it is highly expressed in different areas of the central nervous system (Gibb and Garthwaite, 2001; Mergia et al., 2003), and that its expression profile coincides with neuronal differentiation (Jurado et al., 2003). Thus, understanding the mechanisms that regulate its expression may help to clarify its role in neuronal development and synaptogenesis (Polleux et al., 2000; Wagenen and Rehder, 2001; Ding et al., 2005). In this study, we have shown that the mRNA transcripts that encode the α_2 subunit of NO-sensitive guanylyl cyclase have a 3′ UTR of at least 1873 bp. Furthermore, we identified several AREs in this region that are targeted by proteins of the *elav* family and AUF1 proteins, involved in stabilising/destabilising mRNA. This structural characteristic has previously not been studied in mRNAs encoding the α_2 subunit, although it has already been shown that mRNAs encoding the α_1 and β_1 subunits have a long 3′ UTR to which stabilising proteins bind (Klöss et al., 2003; Klöss et al., 2004). Furthermore, our results demonstrate that expression of the α_2 subunit of NO-sensitive guanylyl cyclase is regulated in granule cells by a mechanism that affects mRNA stability. The regulation of mRNA decay is an important means to control gene expression (Guhaniyogi and Brewer, 2001) and it has been seen to apply to several components of the NO-cGMP pathway (Rodríguez-Pascual et al., 2000; Pérez-Sala et al., 2001; Klöss et al., 2003; Klöss et al., 2004). Although we cannot rule out an increase in α_2 mRNA transcription in the presence of NMDA, the almost 3.5-fold increase in α_2 mRNA accumulation induced by NMDA in the presence of

actinomycin D suggests that the rate of mRNA degradation is lowered by NMDA. It was somewhat surprising that cycloheximide, long recognised for its ability to inhibit protein synthesis, produced a threefold increase in the levels of α_2 mRNA, and that NMDA did not produce any additional effect under these conditions. These results suggest that both cycloheximide and NMDA share the mechanism by which they increase the levels of α_2 mRNA, and imply that these mRNA transcripts are more stable under these conditions. This is further supported by the fact that the inhibition of protein synthesis increases mRNA stability in several different systems (Altus et al., 1987; Oliveira and McCarthy, 1995; Ross, 1995), mainly in relation to mRNA transcripts that contain AU-rich elements (AREs) (Guhaniyogi and Brewer, 2001) such as α_2 mRNA. Cycloheximide is thought to interact with some aspects of mRNA translation itself, elements that are coupled to the activation of ARE-mRNA degradation (Savant-Bhonsale and Cleveland, 1992).

To date, there are three ARE-binding proteins that reportedly are involved in regulating rapid mRNA decay in vivo: HuR (Ma et al., 1996), tristetraprolin (TTP) (Carballo et al., 2000), and the poly(U)-binding and degradation factor AUF1 (also known as hnRNP D) (Brewer, 1991; Wagner et al., 1998). We found that nuclear protein extracts from granule cells bound in vitro to RNA probes that corresponded to the α_2 mRNA 3′ UTR. Although these experiments did not offer any information regarding the identity of the proteins bound to this RNA, we know that they are concentrated in the nucleus. Moreover, even though this technique does not allow the intensity of the band corresponding to the RNA-protein complexes to be accurately quantified, there was a clear reduction in the intensity of the complex when the RNA probe was incubated with nuclear extracts from NMDA-treated cell. Hence, it appears that NMDA treatment causes a decrease in the amount of the protein that associates with this RNA or it favours their displacement. In conjunction, the identification of α_2 mRNA transcripts in complexes immunoprecipitated with an anti AUF1 antibody show that these destabilising factors do indeed bind to the α_2 mRNA. The amount of the four AUF1 isoforms bound is reduced by about 50% in the cells incubated with NMDA. As a consequence, one would expect ARE-containing mRNAs to be stabilised – as demonstrated for the β-adrenergic receptor mRNA whose stability is controlled by alterations in the levels of AUF1 (Pendel et al., 1996). Immunoprecipitation studies also provided evidence for the binding of Hu proteins to α_2 mRNA, which was present in complexes immunoprecipitated with an anti-HuR antibody (which also recognises HuB, HuC, HuD as well as HuR). Hence, these α_2 mRNA transcripts can bind both stabilising and destabilising proteins. It has been shown that the binding of HuR and AUF1 to a target transcript may occur in a competitive fashion (Lal et al., 2004). Thus, we cannot rule out the possibility that the decrease in the amount of AUF1 leads to an increase in the formation of Hu-mRNA complexes. The binding of HuR to RNA probes synthesised from the 3′ UTR of α_1 and β_1 mRNAs has been previously observed in smooth muscle cells (Klöss et al., 2003; Klöss et al., 2004). Hence, the mechanism controlling the decay of guanylyl cyclase subunit mRNA may be widespread to regulate guanylyl cyclase activity and might explain the accumulation of α_1, β_1 and α_2 mRNA induced by NMDA already observed by us (Jurado et al., 2003). Moreover, the reduction in AUF1 protein levels may affect the stability of many different mRNAs and might provide a means by which NMDA regulates gene expression.

Exposure to NMDA provokes a decrease in the levels of AUF1 and an increase in the accumulation of α_2 mRNA by a mechanism that depends on synthesis of cGMP and cGK activation. This mechanism is tonically active in control cells, and NMDA stimulates it. This conclusion is supported by the fact that, both the increase in α_2 mRNA and the decrease in AUF1 levels caused by NMDA treatment were effectively prevented by pre-treatment with specific inhibitors of the NO-sensitive guanylyl cyclase and of cGK and, because cGK inhibition in non-NMDA stimulated cells caused an increase in AUF1 levels, an a reduction in the amount of α_2 mRNA. Moreover, pre-treatment with the cGMP analogue Sp-8-Br-PET-cGMPS that activates cGK, also caused a reduction in the levels of AUF1 and an increase in the amount of α_2 mRNA comparable with that induced by NMDA. We demonstrated that stimulation with NMDA produced an increase in NO, which in turn activated cGMP synthesis by guanylyl cyclase. It appeared that the produced cGMP binds to and activates cGK, because the phosphorylation of two well-known substrates of this enzymatic activity (VASP and CREB) increased. Although the mechanism by which cGK regulates AUF1 levels remains unclear, one possibility is that cGK suppresses the expression of AUF1 proteins by phosphorylation of CREB or of another transcription factor. Indeed, the influence of PKG on gene expression has been demonstrated in different cell types, including neurons (Gudi et al., 1999; Fujiwara et al., 2002; L'Etoile et al., 2002; Smolenski et al., 2004; Pilz and Broderick, 2005), and in some cases this activity is clearly mediated by CREB phosphorylation (Ciani et al., 2002; Chen et al., 2003; Chan et al., 2004). Based on the data presented here, we hypothesise that NMDA stimulation decreases the amount of AUF1 in granule cells and, as a consequence, stabilises different mRNAs that are targeted by these proteins.

Materials and Methods

Cell culture

All procedures relating to the care of animals were conducted according to institutional ethical guidelines for animal experiments and following the regulations of the European Council Directive (86/609/EEC). Primary dissociated cerebellar cultures were established using cerebellar tissue from 7-day-old (P7) male or female Wistar albino rat pups, according to the methods described previously (Baptista et al., 1994; Brewer, 1995) with minor modifications (Jurado et al., 2003). Cerebellar cells were diluted in Neurobasal A supplemented with B27 (GIBCO BRL, Uxbridge, UK), 20 mM KCl, 0.5 mM glutamine and the stabilised antibiotic antimycotic solution (SIGMA). The cells were seeded onto coverslips, 96-well, or 6-well tissue culture plates pre-coated with poly-L-lysine at a density of 100×10^5 cell/coverslip, 200×10^5 cell/well or 5×10^6 cells/well, respectively. The cultures were maintained in a humidified incubator at 5% CO_2, 37°C and after 24 hours in culture, 10 μM cytosine-β-D-arabinofuranoside (final concentration) was added to each well to inhibit the proliferation of non-neuronal cells. This culture medium is optimised for neuronal survival and minimal glial proliferation, and more than 95% of the cells expressed neuronal markers after 48 hours of culture. The cells were maintained in culture and the experiments were performed after 7 days in vitro (7-DIV).

RNA isolation and quantification

After subjecting 7-DIV cells to the appropriate treatment, total RNA was extracted from cells using the RNeasy kit (Quiagen GmbH, Hilden, Germany) and the RNA was quantified using the RiboGreen™ RNA Quantification Kit (Molecular Probes Invitrogen, Barcelona, Spain) as previously described (Ferrero and Torres, 2002).

Reverse transcriptase (RT)-PCR and real-time RT-PCR reactions

RT-PCR reactions were performed in two steps as described previously (Jurado et al., 2003). First strand cDNAs were synthesised in RT buffer containing 5.5 mM

$MgCl_2$, 500 μM per dNTP, 2.5 μM random hexamers, 0.4 U/ml RNAse inhibitor and 3.125 U/ml MultiScribe™ RT (Applied Biosystems). The reactions were performed in a final volume of 50 μl containing 1 μg of RNA and an incubation step of 10 minutes at 25°C to maximise primer-RNA-template binding. The reverse transcription reaction was performed at 48°C for 30 minutes and reverse transcriptase was inactivated before the PCR reactions by heating the samples at 95°C for 5 minutes. The specific PCR primers and the probe for the guanylyl cyclase α_2 subunit were designed using the published sequence (accession number AF109963 and NM_023956) (Koglin and Behrends, 2000) with the help of the primer express software package (Applied Biosystems, Madrid, Spain). Forward primer, position 828 5′-TCT GCA GAC CAT TCC AAC AAA G-3′; reverse primer, position 941 5′-TCC TCA CCA AAC CTC TCT TGA ATT-3′; TaqMan® probe, position 907 5′-(FAM)-TCA GTC CGA GTA CAT TTG CAG TAC ACC GAA-(TAMRA)-3′. 18S rRNA was used as the endogenous control. To amplify a 200 bp fragment, we used a commercial mixture of primers and TaqMan probe labelled with VIC and TAMRA at the 5′ and 3′ end, respectively (Applied Biosystems). PCR reactions were followed in an ABI PRISM 7700 Sequence Detection System (Applied Biosystems) with TaqMan Gold PCR reagents. The reaction mixture contained TaqMan PCR buffer, 5.5 mM $MgCl_2$, 200 μM dATP, 200 μM dCTP, 200 μM dGTP, 400 μM dUTP, 0.025 U/μl AmpliTaq Gold DNA polymerase, 0.01 U/μl AmpErase UNG, 300 nM of each primer and 300 nM of TaqMan probe. Reactions were performed with an initial incubation at 50°C for two minutes followed by 10 minutes at 95°C for AmpliTaq Gold activation and 40 cycles (melting 95°C for 15 seconds, annealing and extension 60°C for 1 minute). Fluorescence was determined at each step of every cycle. Quantifications were always normalised using endogenous control 18S rRNA to check for variability in the initial concentrations, the quality of the total RNA and the conversion efficiency of the reverse transcription reaction.

mRNA decay assay

The decay rate of α_2 mRNA was measured in an actinomycin D time-course assay. Briefly, transcription was inhibited in control or NMDA-treated cells by adding actinomycin D (10 μg/ml) to the culture medium, and RNA samples were harvested at selected time points thereafter. The relative abundance of α_2 mRNA was determined by quantitative RT-PCR as described before.

Intracellular Ca^{2+} measurements

Increases in intracellular Ca^{2+} were determined using the FLUOstar OPTIMA fluorescence microplate reader equipped with two injectors (BMG LabTechnologies, Offenburg, Germany). Granular neurons maintained in culture for 7-DIV were loaded with 4 μM Fluo-4 acetoxy methylester (Fluo-4 AM) in Locke's buffer for 45 minutes at 37°C, and they were subsequently washed twice with fresh Locke's buffer before further incubating for 15 minutes. All experiments were performed at 37°C and the data collected at 0.5 or 1 seconds intervals. The initial volume in each well was 48 μl of Mg^{2+}-free Locke's buffer. Fluorescence was excited using a 485 nm filter and read through a 520 nm long-pass emission filter. To measure Ca^{2+} responses in cells, the baseline fluorescence was first monitored for 5 seconds, then cells were stimulated with 100 μM NMDA (final concentration) and fluorescence monitored for up to 35 seconds. At the end of each measurement, 0.1% Triton X-100 (final concentration) was added to each well to permeate cells and the maximal fluorescence in each well measured (F_{max}). Finally, EGTA-Tris was added and the minimal fluorescence (F_{min}) in each well was measured. To calibrate the response the following equation was used to determine the intracellular free Ca^{2+} concentration $[Ca^{2+}]_i=k_d\,[F\text{-}F_{min}]/[F_{max}\text{-}F]$, using K_d=345 nM for Fluo-4. Each well was calibrated using its own F_{max} and F_{min} readings.

NO measurements

NO was measured using the FLUOstar OPTIMA fluorescence microplate reader equipped with two injectors (BMG LabTechnologies, Offenburg, Germany). Cells plated on 96-well polylysine-coated plates and maintained in culture for 7-DIV were loaded with 10 μM DAF-FM diacetate for 45 minutes at room temperature in Locke's buffer. Fluorescence was recorded using 495 nm excitation and 515 nm emission filters. Basal fluorescence (F_0) was first monitored for 5 seconds, before NMDA 100 μM (final concentration) was injected and the fluorescence recorded for an additional 25 seconds (data were collected at 1 second intervals). After this time period, DEA/NO (~80 μM final concentration) was added and the fluorescence monitored for an additional 10 seconds. Incubation with L-NAME was performed during DAF-FM loading. F/F_0 was calculated for each time point and presented versus time. Although DAF-FM has been shown to be more photostable than DAF-2 it should bear in mind that the fluorescence of the NO adduct of DAF-2 is enhanced by Ca^{2+} and light, making it difficult to compare different measurements performed in different conditions (Broillet et al., 2001).

Immunocytochemistry

Cerebellar granule cells were plated on polylysine-coated coverslips at a density of 200,000 cell/coverslip. Cells were stimulated with 100 μM NMDA in Locke's buffer for 2 minutes and then fixed for 15 minutes in 4% paraformaldehyde freshly prepared in 0.1 M phosphate buffer pH 7.4. The cells were then washed twice with TBS, (5 minutes each), and the coverslips were incubated with blocking buffer (TBS containing 0.2% Triton X-100, 10% normal donkey serum). The cells were washed twice more for 5 minutes with TBS and then incubated for 24 hours at 4°C with the primary sheep anti-formaldehyde-fixed cGMP antibody (1:4000; kindly provided by Jan de Vente) diluted in TBS containing 1% normal donkey serum and 0.2% Triton X-100. After washing three times (5 minutes each) with TBS containing 0.1% Triton X-100, the coverslips were incubated with Cy™2-conjugated affinity-purified donkey anti-sheep IgG (H+L; 1:200 in TBS; Jackson ImmunoResearch, West Grove, PA). After several washes in TBS, the coverslips were mounted with prolong antifade (Molecular Probes) and the cells were viewed with a Nikon Diaphot microscope equipped with a 40×1.3 N.A oil immersion fluor objective, a mercury lamp light source and fluorescein Nikon filter sets.

Fractionation of granule cells and mobility-shift assays

Whole-cell lysates from control or NMDA-treated granule cells (100 μM, 24 hours) were prepared by scraping PBS-washed cells in ice-cold lysis buffer (20 mM Hepes, pH 7.9, 400 mM NaCl, 1 mM EDTA, 1 mM EGTA, 1 mM DTT, 0.5% NP-40, containing protease inhibitors: 1 mM AEBSF, 0.8 μM aprotinin, 50 μM Bestatin, 15 μM E-64; 20 μM leupeptin and 10 μM pepstatin A). The cell debris was cleared from the cell lysates by centrifugation at 14,000 ***g*** for 5 minutes at 4°C in a Heraeus Microfuge, and the protein concentration in the supernatants determined by the microBradford assay (Bio-Rad). Nuclear and cytoplasmic fractions were prepared according to a procedure described previously (Schreiber et al., 1989). Briefly, cells were washed once with ice-cold PBS and scraped in the same medium. Upon centrifugation they were resuspended in 10 mM Hepes pH 7.9, 10 mM KCl, 0.1 mM EDTA, 0.1 mM EGTA, 1 mM dithiothreitol (DTT), 1 mM AEBSF, 0.8 μM aprotinin, 50 μM Bestatin, 15 μM E-64; 20 μM leupeptin and 10 μM pepstatin A. After 15 minutes incubation on ice, Nonidet P-40 was added to a final concentration of 0.5% and cells were vortexed for 10 seconds before pelleting the nuclei by centrifugation for 5 minutes at 14,000 ***g***. After removing the supernatant (cytoplasmic fraction) the nuclear pellets were extracted by shaking on ice for 45 minutes in 50 μl of 20 mM Hepes pH 7.9, 400 mM NaCl, 1 mM EDTA, 1 mM EGTA, 1 mM DTT, and protease inhibitors as above. After centrifugation at 14,000 ***g*** for 5 minutes, the protein content was determined using the Bradford method (Bio-Rad) and subjected to electrophoresis or stored at –70°C.

The 3′ UTR of the rat guanylyl cyclase α_2 subunit mRNA was cloned by RT-PCR as follows. Total RNA was extracted from 7-DIV cells and reverse transcribed with Oligo-dT and MultiScribe™ RT (Applied Biosystems) in RT buffer containing 5.5 mM $MgCl_2$, 500 mM per dNTP, 2.5 μM OligodT, 0.4 U/ml RNase inhibitor and 3.125 U/ml MultiScribe™ RT. Reactions were performed in a final volume of 50 μl containing 1 μg RNA with an incubation step of 10 minutes at 25°C, 30 minutes at 48°C and finally 5 minutes at 95°C to inactivate the reverse transcriptase before the PCR reaction. The following oligodeoxynucleotides were used to amplify two different regions of the α_2 subunit 3′-UTR: 5′-CTCCGGGAAACTAGCCTCTG-AGA-3′ (upstream) and 5′-ATACAGAAAAAATGGAATTTTCTAGTAGAAC-3′ (downstream) used to amplify a 843 bp fragment and 5′-TTAGTGATTAG-TGCTTGAGCTGAGA-3′ (upstream) and 5′-CCTGGGTATTCCTAGGCAGCTT-3′ (downstream) to amplify a 1176 bp fragment. The PCR reaction mixture contained TaqMan PCR buffer, 5.5 mM $MgCl_2$, 200 μM dATP, 200 μM dCTP, 200 μM dGTP, 400 μM dUTP, 0.025 U/μl AmpliTaq Gold® DNA polymerase, 300 nM of each primer, 5 μl of cDNA from the previous RT reaction. The PCR reactions were performed in a final volume of 50 μl with an initial incubation at 95°C for 10 minutes to activate the AmpliTaq Gold, and over 40 cycles (melting 60 seconds at 94°C, followed by 30 seconds at 62°C for annealing and 90 seconds at 70 °C for elongation) with a final elongation of 7 minutes at 68°C. The PCR products were sequenced (3730 DNA Analyzer, Applied Biosystems, Madrid, Spain), and verified by restriction mapping and sequencing.

The RNA probes were transcribed as follows. Two micrograms of DNA (linearised or PCR fragments) were added to transcription buffer, which consisted of 40 mM Tris-HCl pH 7.9, 6 mM $MgCl_2$, 10 mM DTT, 2 mM spermidine, 10 mM NaCl, 1 mM ATP, CTP and GT, 10 U RNasin (Promega, Madison, WI), 2 μl of [α^{32}P]UTP to give a final reaction volume of 20 μl, and 20 U T7 RNA polymerase (Promega, Madison, WI). The reactions were carried out for 1 hour at 37°C. Three units of DNase I (Promega, Madison, WI) were added to the samples and incubated for an additional 45 minutes at 37°C. The radiolabelled RNA probes were purified in Sephadex G-50 Quick Spin Columns (Roche) and the radiolabelled transcripts were analysed by electrophoresis to estimate the yield and specific activity. The radioactivity incorporated into the transcripts was usually higher than 80% and the specific activity ranged from 0.2 to 0.5 μCi/pmol.

For the binding experiments, nuclear or cytosolic extracts (2 μg per lane) prepared from control or NMDA-treated cells were incubated in 10 mM Tris-HCl pH 7.4, 50 mM NaCl, 1 mM $MgCl_2$, 0.5 mM EDTA, 5 mM DTT, 5% glycerol, and containing 0.2 mg/ml of tRNA (Pharmacia) as competitor with approximately 0.3 pmol (65,000 cpm) of the respective probe. After 15 minutes at room temperature, 6 U of RNase T1 were added for 20 minutes to digest the unbound RNA. RNA-protein complexes were resolved by non-denaturing 5% polyacrylamide gel in 0.25× Trisborate-EDTA buffer and visualised by autoradiography.

Western blotting

The indicated cellular protein extracts were separated on 10% or 12% SDS-polyacrylamide gels and electrophoretically transferred to polyvinylidene difluoride (PVDF) membranes. After blocking non-specific binding sites with 3% bovine serum albumin (BSA; SIGMA) in Tris-saline buffered (TBS) containing 0.05% Tween-20 at room temperature for 1 hour, the membranes were incubated with: anti-VASP rabbit polyclonal (1:2000) that recognises both a 46 kDa (Ser157 dephosphorylated) and 50 kDa (Ser157 phosphorylated) form of VASP (Calbiochem); anti-Lamin B1 (0.1 μg/ml) (ab16048; abcam), anti-GAPDH (monoclonal antibody against glyceraldehyde-3-phosphate dehydrogenase, clone 6C5 Ambion) or the anti-AUF1 rabbit polyclonal IgG (1 μg/ml) that recognises AUF1 isoforms of Mr 37, 40,42 and 45 (Upstate). Proteins were visualised using a goat anti-rabbit secondary antibody conjugated to horseradish peroxidase (HRP) and a chemiluminiscence detection system. Chemiluminescence was detected directly by using a Bio-Rad Fluor S instrument and analysed with Bio-Rad Quantity One software (BIORAD, Hercules, CA).

Immunoprecipitation assays

Immunoprecipitation (IP) of endogenous RNA-protein complexes was performed as previously described (Lal et al., 2004) with minor modifications. Nuclear (75-100 μg) or cytoplasmic (400-430 μg) protein extracts were incubated (1 hour, 4°C) with a 50% (v/v) suspension of Protein-A-agarose beads (Sigma) pre-coated with 30 μg of rabbit IgG (Sigma), anti-AUF1 (Upstate) or anti-HuR (H-280, which detects HuR, HuB, HuC and HuD, Santa Cruz Biotech) antibodies. The beads were then washed three times using NT2 buffer (50 mM Tris-HCl pH 7.4, 150 mM NaCl, 1 mM $MgCl_2$ and 0.05% NP-40).

To analyse the RNA in the IP complexes, the beads were incubated with 100 μl NT2 buffer containing 20 U RNase-free DNase I (Sigma) for 15 minutes at 30 °C. They were then washed with NT2 buffer and further incubated in 100 μl NT2 buffer containing 0.1% SDS and 50 μg proteinase K (15 minutes, 55°C). The RNA was extracted using the RNeasy mini Kit and then, RT-PCR and real-time RT-PCR were performed. The RNA isolated was reverse transcribed using random hexamers and the resulting material was used for PCR amplification using gene-specific primer pairs as described before. As a negative control, 50% of the RNA was incubated without MultiScribe™ RT. Control 18S rRNA, which is not a target of either RNA binding protein (RBP), was used to monitor the background levels of RNA in the IP complexes.

Statistical analysis

The results are expressed as means ± s.e.m. of three or more experiments. The data were analysed by one-way ANOVA followed by Bonferroni's test (confidential interval 95%). The differences between the means were considered statistically significant when $P<0.05$.

This study was financed by a grant from the Ministerio de Educación y Ciencia (BFI2003-00731). S.J. was supported by a fellowship from the same source. We thank J. de Vente for providing us with the anti-cGMP antibody and M. Sefton for linguistic assistance.

References

Akamatsu, W., Okano, H. J., Osumi, N., Inoue, T., Nakamura, S., Sakakibara, S.-L., Miura, M., Matsuo, N., Darnell, R. B. and Okano, H. (1999). Mammalian ELAV-like neuronal RNA-binding proteins HuB and HuC promote neuronal development in both the central and the peripheral nervous system. *Proc. Natl. Acad. Sci. USA* **96**, 9885-9890.

Altus, M. S., Pearson, D., Horiuchi, A. and Nagamine, Y. (1987). Inhibition of protein synthesis in LLC-PK1 cells increases calcitonin-induced plasminogen-activator gene transcription and mRNA stability. *Biochem. J.* **242**, 387-392.

Baader, S. L. and Schilling, K. (1996). Glutamate receptors mediate dynamic regulation of nitric oxide synthase expression in cerebellar granule cells. *J. Neurosci.* **16**, 1440-1449.

Balazs, R., Jorgensen, O. S. and Hack, N. (1988). N-Methyl-D-aspartate promotes the survival of cerebellar granule cells in culture. *Neuroscience* **27**, 437-451.

Baptista, C. A., Hatten, M. E., Blazeski, R. and Mason, A. (1994). Cell-cell interactions influence survival and differentiation of purified Purkinje cells in vitro. *Neuron* **12**, 243-260.

Bessho, Y., Nawa, H. and Nakanishi, S. (1994). Selective up-regulation of an NMDA receptor subunit mRNA in cultured cerebellar granule cells by K(+)-induced depolarization and NMDA treatment. *Neuron* **12**, 87-95.

Bhattacharya, S., Giordano, T., Brewer, G. and Malter, J. S. (1999). Identification of AUF-1 ligands reveals vast diversity of early response gene mRNAs. *Nucleic Acid Res.* **27**, 1464-1472.

Bredt, D. S. and Snyder, S. H. (1994). Transient nitric oxide synthase neurons in embryonic cerebral cortical plate, sensory ganglia, and olfactory epithelium. *Neuron* **13**, 301-313.

Brenman, J. E., Chao, D. S., Gee, S. H., McGee, A. W., Craven, S. E., Santillano, D. R., Wu, Z., Huang, F., Xia, H., Peters, M. F. et al. (1996). Interaction of nitric oxide synthase with the postsynaptic density protein PSD-95 and alpha1-syntrophin mediated by PDZ domains. *Cell* **84**, 757-767.

Brewer, G. (1991). An A + U-rich element RNA-binding factor regulates c-myc mRNA stability in vitro. *Mol. Cell. Biol.* **11**, 2460-2466.

Brewer, G. (1995). Serum-free B27/neurobasal medium supports differentiated growth of neurons from the striatum, substantia nigra, septum, cerebral cortex, cerebellum, and dentate gyrus. *J. Neurosci. Res.* **42**, 674-683.

Broillet, M. C., Randin, O. and Chatton, J.-Y. (2001). Photoactivation and calcium sensitivity of the fluorescent NO indicator 4,5-diaminofluorescein (DAF-2): implications for cellular NO imaging. *FEBS Lett.* **491**, 227-232.

Carballo, E., Lai, W. S. and Blackshear, P. J. (2000). Evidence that tristetraprolin is a physiological regulator of granulocyte-macrophage colony-stimulating factor messenger RNA deadenylation and stability. *Blood* **95**, 1891-1899.

Chan, S. H., Chang, K. F., Ou, C. C. and Chan, J. Y. (2004). Nitric oxide regulates c-fos expression in nucleus tractus solitarii induced by baroreceptor activation via cGMP-dependent protein kinase and cAMP response element-binding protein phosphorylation. *Mol. Pharmacol.* **65**, 319-325.

Chen, C. Y. and Shyu, A.-B. (1995). AU-rich elements: characterization and importance in mRNA degradation. *Trends Biochem. Sci.* **20**, 465-470.

Chen, Y., Zhuang, S., Cassenaer, S., Casteel, D. E., Gudi, T., Boss, G. R. and Pilz, R. B. (2003). Synergism between calcium and cyclic GMP in cyclic AMP response element-dependent transcriptional regulation requires cooperation between CREB and C/EBP-beta. *Mol. Cell. Biol.* **23**, 4066-4082.

Ciani, E., Guidi, S., Bartesaghi, R. and Contestabile, A. (2002). Nitric oxide regulates cGMP-dependent CREB phosphorylation and Bcl-2 expression in cerebellar neurons: implication for a survival role of nitric oxide. *J. Neurochem.* **82**, 1282-1289.

Contestabile, A. (2000). Roles of NMDA receptor activity and nitric oxide production in brain development. *Brain Res. Brain Res. Rev.* **32**, 476-509.

Craven, S. E. and Bredt, D. S. (1998). PDZ proteins organize synaptic signalling pathways. *Cell* **93**, 495-498.

Dawson, V. L., Dawson, T. M., Bartley, D. A., Uhl, G. R. and Snyder, S. H. (1993). Mechanism of nitric oxide-mediated neurotoxicity in primary brain cultures. *J. Neurosci.* **13**, 2651-2661.

Ding, J.-D., Burette, A. and Weinberg, R. J. (2005). Expression of soluble guanylyl cyclase in rat cerebral cortex during postnatal development. *J. Comp. Neurol.* **485**, 255-265.

Fan, X. C. and Steitz, J. A. (1998). HNS, a nuclear-cytoplasmic shuttling sequence in HuR. *Proc. Natl. Acad. Sci. USA* **95**, 15293-15298.

Ferrero, R. and Torres, M. (2002). Prolonged exposure of chromaffin cells to nitric oxide down-regulates the activity of soluble guanylyl cyclase and corresponding mRNA and protein levels. *BMC Biochem.* **3**, 26.

Ferrero, R., Rodríguez-Pascual, F., Miras-Portugal, M. T. and Torres, M. (2000). Nitric oxide-sensitive guanylyl cyclase activity inhibition through cyclic GMP-dependent dephosphorylation. *J. Neurochem.* **75**, 2029-2039.

Fujiwara, M., Sengupta, P. and McIntire, S. L. (2002). Regulation of body size and behavioral state of C. elegans by sensory perception and the EGL-4 cGMP-dependent protein kinase. *Neuron* **36**, 1091-1102.

Garthwaite, J. and Boulton, C. L. (1995). Nitric oxide signalling in the central nervous system. *Annu. Rev. Physiol.* **57**, 683-706.

Garthwaite, J., Garthwaite, G. and Hajos, F. (1986). γ-Aminobutyric acid affects the developmental expression of neuron-associated proteins in cerebellar granule cell culture. *J. Neurochem.* **46**, 1256-1262.

Gibb, B. J. and Garthwaite, J. (2001). Subunits of the nitric oxide receptor, soluble guanylyl cyclase, expressed in rat brain. *Eur. J. Neurosci.* **13**, 539-544.

Gudi, T., Hong, G. K., Vaandrager, A. B., Lhomann, S. M. and Pilz, R. B. (1999). Nitric oxide and cGMP regulate gene expression in neuronal and glial cells by activating type II cGMP-dependent protein kinase. *FASEB J.* **13**, 2143-2152.

Guhaniyogi, J. and Brewer, G. (2001). Regulation of mRNA stability in mammalian cells. *Gene* **265**, 11-23.

Holscher, C. (1997). Nitric oxide, the enigmatic neuronal messenger: its role in synaptic plasticity. *Trends Neurosci.* **20**, 298-303.

Jurado, S., Sánchez-Prieto, J. and Torres, M. (2003). Differential expression of NO-sensitive guanylyl cyclase subunits during the development of rat cerebellar granule cells: regulation via N-methyl-D-aspartate receptors. *J. Cell Sci.* **116**, 3165-3175.

Jurado, S., Sánchez-Prieto, J. and Torres, M. (2004). Elements of the nitric oxide/cGMP pathway expressed in cerebellar granule cells: biochemical and functional characterisation. *Neurochem. Int.* **45**, 833-843.

Kleinschmidt, A., Bear, M. F. and Singer, W. (1987). Blockade of NMDA receptors disrupts experience-dependent plasticity of kitten striate cortex. *Science* **238**, 355-358.

Klöss, S., Furneaux, H. and Mülsch, A. (2003). Post-transcriptional regulation of soluble guanylyl cyclase expression in rat aorta. *J. Biol. Chem.* **278**, 2377-2383.

Klöss, S., Srivastava, R. and Mülsch, A. (2004). Down-regulation of soluble guanylyl cyclase expression by cyclic AMP is mediated by mRNA-stabilizing protein HuR. *Mol. Pharmacol.* **65**, 1440-1451.

Koglin, M. and Behrends, S. (2000). Cloning and functional expression of the rat α_2 subunit of soluble guanylyl cyclase. *Biochim. Biophys. Acta* **1494**, 286-289.

Lal, A., Mazan-Mamczarz, K., Kawai, T., Yang, X., Martindale, J. L. and Gorospe, M. (2004). Concurrent versus individual binding of HuR and AUF1 to common labile target mRNAs. *EMBO J.* **23**, 3092-3102.

L'Etoile, N. D., Coburn, C. M., Eastham, J., Kistler, A., Gallegos, G. and Bargmann, C. L. (2002). The cyclic GMP-dependent protein kinase EGL-4 regulates olfactory adaptation in C. elegans. *Neuron* **36**, 1079-1089.

Ma, W. J., Cheng, S., Campbell, C., Wright, A. and Furneaux, H. (1996). Cloning

and characterization of HuR, a ubiquitously expressed Elav-like protein. *J. Biol. Chem.* **271**, 8144-8151.

Meier, E. and Jorgensen, O. S. (1986). Gamma-aminobutyric acid affects the developmental expression of neuron-associated proteins in cerebellar granule cell culture. *J. Neurochem.* **45**, 1256-1262.

Mergia, E., Russwurm, M., Zoidl, G. and Koesling, D. (2003). Major occurrence of the new $\alpha_2\beta_1$ isoform of NO-sensitive guanylyl cyclase in brain. *Cell. Signal.* **15**, 189-195.

Oliveira, C. C. and McCarthy, J. E. G. (1995). The relationship between eukaryotic translation and mRNA stability: a short upstream open reading frame strongly inhibits translational initiation and greatly accelerates mRNA degradation in the yeast *Saccharomyces cerevisiae. J. Biol. Chem.* **270**, 8936-8943.

Pearce, I. A., Cambray-Deakin, M. A. and Burgoyne, R. D. (1987). Glutamate acting on NMDA receptors stimulates neurite outgrowth from cerebellar granule cells. *FEBS Lett.* **233**, 143-147.

Pendel, A., Tremmel, K. D., DeMaria, C. T., Blaxall, B. C., Minobe, W. A., Sherman, J. A., Bisognano, J. D., Bristow, M. R., Brewer, G. and Port, J. D. (1996). Regulation of the mRNA-binding protein AUF1 by activation of the β-adrenergic receptor signal transduction pathway. *J. Biol. Chem.* **271**, 8493-8501.

Peng, S. S.-Y., Chen, C.-Y. A., Xu, N. and Shyu, A.-B. (1998). RNA stabilization by the AU-rich element binding protein, HuR, an ELAV protein. *EMBO J.* **17**, 3461-3470.

Pérez-Sala, D., Cernuda-Morollon, E., Díaz-Cazorla, M., Rodríguez-Pascual, F. and Lamas, S. (2001). Posttranscriptional regulation of human iNOS by the NO/cGMP pathway. *Am. J. Physiol. Renal Physiol.* **280**, F466-F473.

Pilz, R. B. and Broderick, K. E. (2005). Role of cyclic GMP in gene regulation. *Front. Biosci.* **10**, 1239-1268.

Polleux, F., Morrow, T. and Ghosh, A. (2000). Semaphorin 3A is a chemoattractant for cortical apical dendrites. *Nature* **404**, 567-573.

Rodríguez-Pascual, F., Hausding, M., Ihrig-Biedert, I., Furneaux, H., Levy, A. P., Förstermann, U. and Kleinert, H. (2000). Complex contribution of the 3′-untranslated region to the expressional regulation of the human inducible nitric-oxide synthase gene. Involvement of the RNA-binding protein HuR. *J. Biol. Chem.* **275**, 26040-26049.

Ross, J. (1995). mRNA stability in mammalian cells. *Microbiol. Rev.* **59**, 423-450.

Russwurm, M., Wittaus, N. and Koesling, D. (2001). Guanylyl cyclase/PSD-95 interaction targeting of the nitric oxide-sensitive $\alpha_2\beta_1$ guanylyl cyclase to synaptic membranes. *J. Biol. Chem.* **276**, 44647-44652.

Sachs, A.-B. (1993). Messenger RNA degradation in eukaryotes. *Cell* **74**, 413-421.

Savant-Bhonsale, S. and Cleveland, D. W. (1992). Evidence for instability of mRNAs containing AUUUA motifs mediated through translation-dependent assembly of a >20S degradation complex. *Genes Dev.* **6**, 1927-1939.

Schreiber, E., Matthias, P., Muller, M. M. and Schaffner, W. (1989). Rapid detection of octamer binding proteins with "mini-extracts", prepared from a small number of cells. *Nucleic Acids Res.* **17**, 6418.

Sheng, M. and Pak, D. T. (2000). Ligand-gated ion channel interactions with cytoskeletal and signalling proteins. *Annu. Rev. Physiol.* **62**, 755-778.

Smolenski, A., Schultess, J., Danielewski, O., Arguinzonis, M. I. G., Thalheimer, P., Kneitz, S., Walter, U. and Lohmann, S. M. (2004). Quantitative analysis of the cardiac fibroblast transcriptome-implications for NO/cGMP signaling. *Genomics* **83**, 577-587.

Virgili, M., Facchinetti, F., Sparapani, M., Tregnago, M., Lucchi, R., Dall'Olio, R., Gandolfi, O. and Contestabile, A. (1998). Neuronal nitric oxide synthase is permanently decreased in the cerebellum of rats subjected to chronic neonatal blockade of N-methyl-D-aspartate receptors. *Neurosci. Lett.* **258**, 1-4.

Wagenen, S. V. and Rehder, V. (2001). Regulation of neuronal growth cone filopodia by nitric oxide depends on soluble guanylyl cyclase. *J. Neurobiol.* **46**, 206-219.

Wagner, B. J., De Maria, C. T., Sun, Y., Wilson, G. M. and Brewer, G. (1998). Structure and genomic organization of the human AUF1 gene: alternative pre-mRNA splicing generates four protein isoforms. *Genomics* **48**, 195-202.

Xu, N., Chen, C. Y. and Shyu, A.-B. (1997). Modulation of the fate of cytoplasmic mRNA by AU-rich elements: key sequence features controlling mRNA deadenylation and decay. *Mol. Cell. Biol.* **17**, 4611-4621.